*Earth's Future*

Supporting Information for

# Detecting Vietnam War Bomb Craters in Declassified Historical KH-9 Satellite Imagery

Philipp Barthelme[1], Eoghan Darbyshire[2], Dominick Spracklen[3], and Gary R Watmough[1,4,5]

[1] School of Geosciences, University of Edinburgh, Edinburgh, United Kingdom.

[2] Conflict and Environment Observatory, Mytholmroyd, United Kingdom.

[3] School of Earth and Environment, University of Leeds, Leeds, United Kingdom.

[4] Global Academy of Agriculture and Food Systems, University of Edinburgh, United Kingdom

[5] Novel Data Ecosystems for Sustainability (NODES) Research Group. Advancing Systems Analysis Program, International Institute for Applied Systems Analysis (IIASA), Austria

## Contents of this file

Text S1: Crater labeling
Text S2: THOR processing
Figure S1: Timeseries of B-52 bombing missions by source database
Figure S2: Geographic distribution of B-52 bombing missions by source database
Table S1: KH-9 images used in the analysis
Table S2: Matching between estimated weapon type weight and weapon type
Table S3: Weapon types used in the analysis
Table S4: Spearman correlation coefficients Quang Tri
Table S5: Spearman correlation coefficients Tri-border area

## Introduction

The following gives additional information about the methods used for crater labeling (Text S1) and the processing of the THOR bombing records (Text S2, Figure S1, Figure S2, Table S2, Table S3). To assess the robustness of the results to the THOR processing, Tables S4 and S5 provide spearman correlations between detected bomb craters and THOR bombing for different subsets of THOR, extending Table 2 in the paper. In addition, Table S1 lists the KH-9 images used during the analysis.

### Text S1. Crater labeling

Simple craters usually consist of a bowl-shaped hole with an elevated rim and a circular continuous ejecta blanket around the rim (Barlow et al., 2021; Roberts et al., 2021). In the KH-9 imagery, crater bowl and rim were usually visible as a bright circle with a shadow on the side of the crater that faces the sun, or as a dark circle if the crater was filled with water. The crater ejecta were often visible as a bright circle around the crater bowl and in some cases as rayed ejecta extending much further from the crater (Sabuwala et al., 2018). We labeled an object as a crater of type *Rim* if both the crater bowl and the crater ejecta were visible and could be distinguished from each other.

In the imagery, small craters were often only visible as circular white blobs, where the crater bowl could not be distinguished from the crater ejecta. We labeled these circular white blobs as craters of type *Pattern* if they appeared in patterns with other blobs of the same size. We also ensured that the context did not indicate them to be different objects such as houses, trees or circular graves. This was done using both the context visible in the KH-9 imagery and, if necessary, current Google Earth imagery. As the image resolution and quality made it difficult to reliably identify very small objects as craters, we excluded all objects smaller than 25 pixels, equivalent to 25 $m^2$. Similar to our approach, Lin et al. (2020) limit their analysis to bomb craters with diameters between 3 and 12 m using satellite imagery with a resolution of 0.5 m. Duncan et al. (2023), who also use imagery with a resolution of 0.5 m, do not set a size limit during crater labeling but find that their model performs worse on smaller craters of less than 30 $m^2$. They also note the difficulty of labeling craters on vegetated and heterogeneous surfaces and limit their study to agricultural fields with short vegetation.

We labeled craters as type *Group* if crater bowls or continuous ejecta of three or more craters overlapped, in which case only the crater bowl was labeled as the crater ejecta could not be attributed clearly to an individual crater. We labeled craters as type *Bowl* if only the crater bowl, often filled with water, was visible. This can occur for older craters where the ejecta has eroded over time. We labeled craters as type *Crescent* where we saw a crescent shaped crater rim/ejecta, which can occur in areas with steep slopes or where erosion has affected the crater appearance (Aschauer & Kenkmann, 2017; Hayashi & Sumita, 2017). Craters of types *Group*, *Bowl* and *Crescent* were difficult to identify reliably, and we often relied on context to make the final decision.

We used the circle shape from the QGIS toolbar to label the craters, even if they were not perfectly circular, as we found this to be an efficient approach. We used freehand label shapes to separate overlapping crater bowls. The labels encompassed both the crater bowl and, if visible, the crater ejecta, but excluded rayed ejecta. For craters of type *Group*, only the crater bowl was labeled since the continuous ejecta could not be attributed clearly to any individual crater. For craters of type *Crescent*, for which a full circular shape is not given, we still used a circle shape as the label, based on the best approximation of the suspected crater shape.

## Text S2. THOR processing

This section provides additional information about issues with the THOR data that we identified during our analysis and describes how we decided to correct or circumvent these issues. This is not an exhaustive list of issues in the THOR data but focuses on the issues that were immediately relevant to our analysis. We chose solutions that were acceptable for the purpose of our research, which compares the bombing on a large scale. However, some individual bombing records might not be processed correctly, which is unavoidable due to the limitations of the THOR data. More work is needed to identify additional limitations, but this was outside the scope of this paper.

1. *Coordinate reference system*

Our analysis suggested that the THOR target coordinates, provided in columns *tgtlatdd_ddd_wgs84* and *tgtlonddd_ddd_wgs84*, despite their names, did not use the WGS84 coordinate reference system but were instead provided in the Indian 1960 geodetic coordinate system (EPSG:4131). We therefore converted these coordinates from EPSG:4131 to EPSG:4326 (using EPSG:1542), which led to a shift of about 500 meters. We found that the resulting coordinates matched the locations of the craters visible in the KH-9 imagery more closely. This was particularly true for B-52 bombing missions where it was often easiest to match the distinct lines of craters to individual records in the THOR data. We also tested the hypothesis using historical topographic maps[1] created by the U.S. Army Map Service during the Vietnam War. These maps show the Military Grid Reference System (MGRS) coordinates, which were used by the U.S. military at the time. While the THOR bombing records do not contain the original MGRS target coordinates, these coordinates are included in the corresponding SEADAB source records available in the National Archives and Records Administration (NARA)

[1] These maps are part of the *AMS Topographic Maps - Series L7014* available at https://maps.lib.utexas.edu/maps/topo/vietnam/ (accessed 21/10/2023)

archives[2]. We again found that the shifted target coordinates matched the MGRS target coordinates more closely when we located those on the topographic maps.

*2. Mission function codes*

We found that multiple mission function descriptions, given in the *mfunc_desc* column in the THOR data, were wrong which, in some cases, also led to a wrong mission function class (*mfunc_desc_class*). We suspected that during the conversion from mission function codes (*mfunc*) to mission function descriptions, the CACTA lookup table was used for both CACTA and SEADAB records. However, some of the code meanings were changed for the SEADAB data, which can be seen in the corresponding NARA documentation[3]. Most notably, B-52 bombing missions were wrongly classified in the THOR data as non-kinetic missions with description "COMBT CARGO AIR  DROP" instead of the correct "HEAVY BOMBARD". The wrong mission functions can be corrected by using the correct lookup table, as provided in the NARA documentation for the SEADAB data, to map the mission function codes (*mfunc*) to the mission function description (*mfunc_desc*). However, we did not use the mission function information in our analysis and therefore did not apply this processing step. We nevertheless make note of this information here as filtering the kinetic records in THOR by using the mission function class has been a common processing step in past analyses. We refer the reader to the corresponding documentation of the SEADAB and CACTA data in the NARA archives for the correct mission function mapping.

*3. B-52 bombing records*

We found that B-52 bombing missions were likely recorded in both the SEADAB and the SACCOACT databases starting from March, 1 1971. Figure S1 shows the number of weapons dropped in B-52 bombing missions by source database. While the SACCOACT and SEADAB records do not match exactly, they approximately agree from early 1971 onwards. We confirmed this by checking individual lines of craters in the KH-9 imagery that often can be matched to both a SEADAB and a SACCOACT B-52 bombing record despite only showing craters for one bomb strike. Notably, the target coordinates from the SACCOACT records

[2] The NARA SEADAB records (National Archives Identifier (NAID): 602566) are available online at https://catalog.archives.gov/id/602566 (accessed 21/10/2023)

[3] p.84-85 in the technical documentation for the NARA SEADAB data (NAID: 602566) https://s3.amazonaws.com/NARAprodstorage/opastorage/live/92/9370/1937092/content/arcmedia/electronic-records/rg-218/seadab/123.1DP.pdf (accessed 21/10/2023) and p.95-96 in the technical documentation of the CACTA data (NAID: 602566) https://s3.amazonaws.com/NARAprodstorage/opastorage/live/45/5547/2554745/content/electronic-records/rg-218/CACTA/136.1DP.pdf (accessed 21/10/2023)

did not exactly match the SEADAB target coordinates. We found that the SACCOACT targets were much less precise and often appeared to be located on a grid of about one nautical mile (approx. 1.8 km). In contrast, the SEADAB targets appeared to be more precise as they more closely matched the lines of craters identified in the KH-9 imagery. This can also be seen in Figure S2, where we compared the spatial distribution of the B-52 bombing missions for the Quang Tri study area. While the numbers aggregated by grid cells (Figure S2a and b) matched well between the databases, Figure S2c and d clearly show the better precision of the SEADAB records. The SEADAB data also appeared to contain additional records for some of the time periods (see Figure S1). We therefore decided to keep the SEADAB records and discarded all SACCOACT records after March, 1 1971.

*4. Missing weapon types in SEADAB*

Many records in the THOR data, including about 1.4 million of the 1.8 million total records originating from the SEADAB database, did not contain information about the weapon type used. As the weapon type information was crucial for our analysis, we imputed some of the missing weapon types based on the estimated weight of the weapon type, which was calculated using the equation

$$weapontypeweight_{est} = \frac{1}{10} \times \frac{weaponsloadedweight}{numweaponsdelivered} \quad (1)$$

where *weaponsloadedweight* describes the weight loaded on the planes flying the mission and *numweaponsdelivered* denotes the total number of weapons loaded on the plane. The imputed weapon types and their corresponding estimated weight are provided in Table S1. However, the estimated weight of a weapon type sometimes matched with multiple potential weapon types. For the cases given in Table S2, this was not an issue as either all the matching weapon types would also be relevant for our analysis (see Section 5) or the number of records for other weapon types were very low. One exception was the estimated weapon type weight of 820 pounds, which matched both the "M117 GP BOMB (750) LD" as well as the "CBU49 AN PR MINE". To allow for a more accurate matching, we took the type of plane into account as we found that the "M117 GP BOMB (750) LD" bombs were more likely to be dropped from one of the following planes: "A-1", "A-37", "B-52", "B-57", "F-100", "F-105" and "F-5". In cases where a different plane was used, we matched the estimated weight of 820 pounds to the "CBU49 AN PR MINE".

*5. Weapon types resulting in large craters*

We selected 22 weapon types for our analysis and discarded all records with other weapon types. The decision was made based on our understanding of which weapon types would result in large craters detectable by our model (≥ 25m$^2$). We also removed some weapon types that might result in large craters but which had very few records associated with them as these did not substantially affect our results. Removing those records made it easier in cases where it was challenging to understand the weapon type from the given name or to impute the weapon type based on its weight. The list of weapon types used for the analysis is given in Table S3.

*6. Maximum of weapons per plane*

We found multiple records with large amounts of weapons dropped that far exceeded the number of weapons that could be carried by the corresponding aircraft. In some cases, this could be traced back to simple typos, but investigating every individual case would be time consuming and often it was unclear if a record could be adjusted or was completely wrong. The maximum number of large bombs an individual plane could carry during the war was 108 (by a B-52 bomber[4]), and as we only considered large bombs in our analysis, we removed all records where the number of weapons per plane exceeded 108. A more sophisticated way to address the issue would be to consider the maximum load of individual aircraft types, but this would be complicated due to the large number of combinations of weapons and aircraft types. Therefore, we opted for this simpler solution which was sufficient for the purpose of our analysis as it removes the most severe errors.

*7. Correlation results for different subsets of the THOR data*

We calculated the correlations between the detected bomb craters and different subsets of the THOR records, aggregated by 2 × 2 km grid cells, in order to test the robustness of the results we presented in the paper (see Tables S4 and S5). As expected, we typically saw higher correlations between craters and bombing records when only considering weapons dropped during the year before the KH-9 images were taken. We also saw higher correlations for the subset of heavier kinetic weapons compared to weapon types weighing less than 200 pounds. Filtering on non-kinetic weapons resulted in much lower correlations, which was expected as these weapon types would not result in craters. Correlations were higher for the B-52 missions recorded in SEADAB compared to the SACCOACT records when considering previous year bombings,

[4] This number corresponds to the B-52D model which was able to carry up to 84 bombs internally and an additional 24 bombs under its wings https://www.nationalmuseum.af.mil/Visit/Museum-Exhibits/Fact-Sheets/Display/Article/195838/the-big-belly-bomber/ (accessed 21/10/2023)

which we suspect was due to the lower precision of the SACCOACT target locations (see Section 3). Overall, the correlation results showed that our analysis was robust and confirmed some of the methods we used for processing the THOR data.

**a. Daily number of bombs dropped on B-52 bombing missions recorded in THOR by source database**

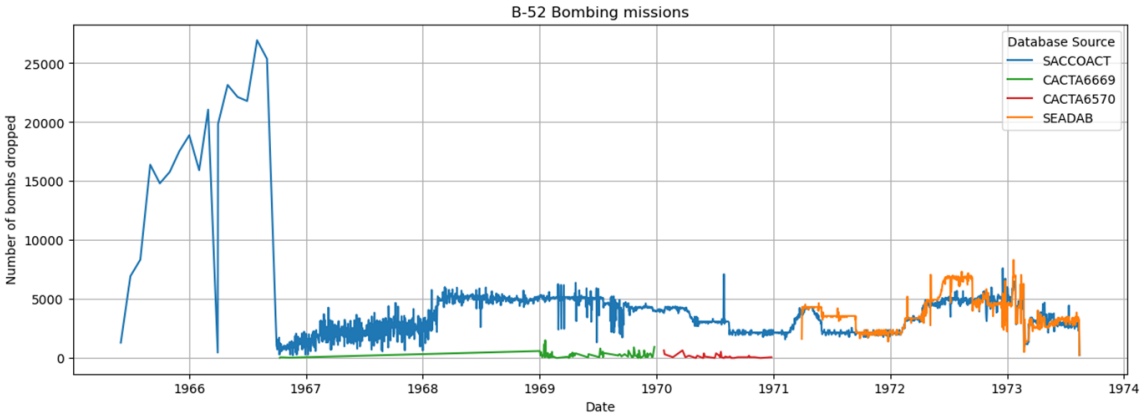


**b. Daily number of bombs dropped on B-52 bombing missions recorded in THOR 1971- 1973**

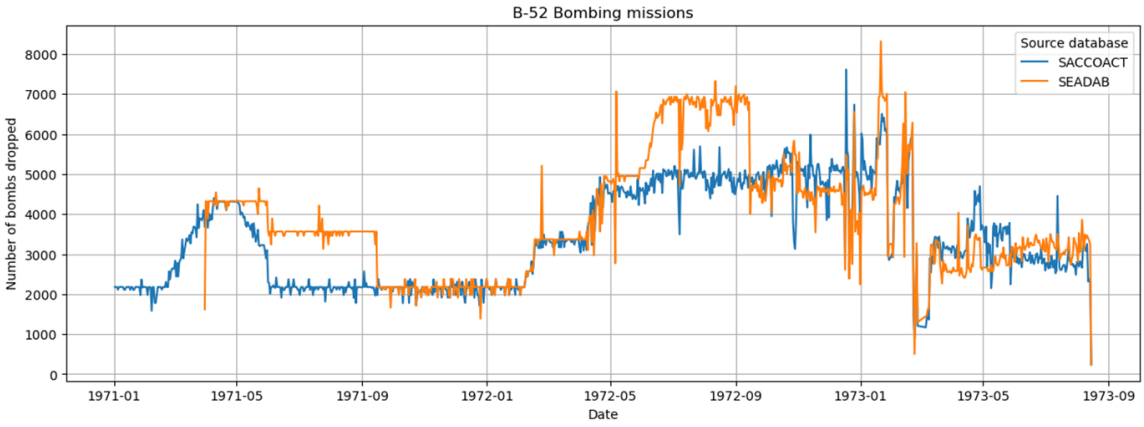


**Figure S1.** Daily number of bombs dropped on B-52 bombing missions by source database, with the full duration shown in (a) and the period after 1971 shown in (b).

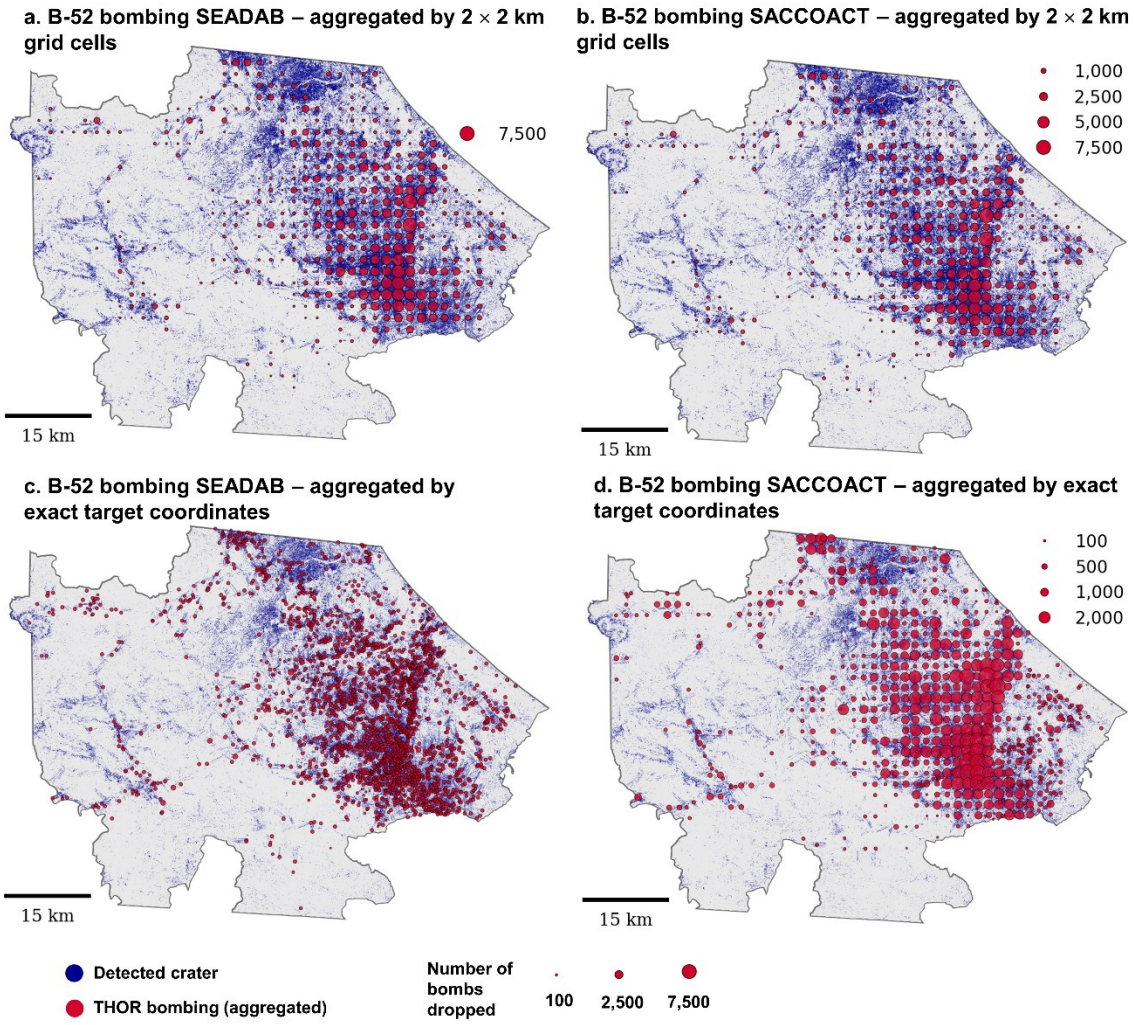


**Figure S2.** B-52 bombing mission during the year before the KH-9 images were taken (March 1972 – March 1973) split up by source database. Panels (a) and (b) show the number of bombs aggregated by a grid of 2 × 2 km whereas (c) and (d) show the number of bombs dropped aggregated by exact target location. The grid pattern visible in panel (d) likely arises from the less precise target locations in the SACCOACT database which lead to multiple records with the exact same target location, often located on a grid of about one nautical mile (~1.8km). However, panel (c) shows that more precise target locations were recorded at the time as they are available in the SEADAB database.

| Entity ID | Study area | Acquisition data |
|---|---|---|
| D3C1205-100113A009 | Quang Tri | 20/03/1973 |
| D3C1205-100113F009 | Quang Tri | 20/03/1973 |
| D3C1205-100113A010 | Quang Tri | 20/03/1973 |
| D3C1205-100113F010 | Quang Tri | 20/03/1973 |
| D3C1205-100113A011 | Quang Tri | 20/03/1973 |
| D3C1205-100113F011 | Quang Tri | 20/03/1973 |
| D3C1205-100113A012 | Quang Tri | 20/03/1973 |
| D3C1205-100113F012 | Quang Tri | 20/03/1973 |
| D3C1204-200292A077 | Tri-border area | 04/11/1972 |
| D3C1204-200292F077 | Tri-border area | 04/11/1972 |
| D3C1204-200292A078 | Tri-border area | 04/11/1972 |
| D3C1204-200292F078 | Tri-border area | 04/11/1972 |
| D3C1204-200292A079 | Tri-border area | 04/11/1972 |
| D3C1204-200292F079 | Tri-border area | 04/11/1972 |
| D3C1204-200292A080 | Tri-border area | 04/11/1972 |
| D3C1204-200292F080 | Tri-border area | 04/11/1972 |
| D3C1204-200292A081 | Tri-border area | 04/11/1972 |
| D3C1204-200292F081 | Tri-border area | 04/11/1972 |
| D3C1204-200292A082 | Tri-border area | 04/11/1972 |
| D3C1204-200292F082 | Tri-border area | 04/11/1972 |

**Table S1.** KH-9 images used in the analysis. Stereo pairs were used during orthorectification but only the aft looking images were used for the crater detection.

| Estimated weapon type weight (in pounds) | Matched weapon type |
|---|---|
| 260 | MK81 GP BOMB (250) |
| 531 | MK 82 GP BOMB (500) LD |
| 571 | MK82 GP BOMB (500) HD |
| 820 | M117 GP BOMB (750) LD/<br>CBU49 AN PR MINE |
| 1100 | MK83 GP BOMB (1000) |

**Table S2.** Matching between estimated weapon type weight and weapon type.

| Weapon type | Source database |
|---|---|
| 500LB GP MK-82 | CACTA |
| 750LB GP M-117 | CACTA |
| 250LB MK-81 | CACTA |
| 500LB GP M-64 | CACTA |
| 250LB M-57 | CACTA |
| 200/260 M81/88 | CACTA |
| 1000LB MK-83 | CACTA |
| 100LB GP M-30 | CACTA |
| 1000LB GP M-65 | CACTA |
| 2000LB MK-84 | CACTA |
| 2000LB M-66 | CACTA |
| 3000LB M-118 | CACTA |
| MK 82 GP BOMB (500) LD | SEADAB |
| M117 GP BOMB (750) LD | SEADAB |
| MK81 GP BOMB (250) | SEADAB |
| MK82 GP BOMB (500) HD | SEADAB |
| MK 82 GP BOMB (500) | SEADAB |
| MK83 GP BOMB (1000) | SEADAB |
| MK82 B | SACCOACT |
| 750 GP | SACCOACT |
| M64A1 | SACCOACT |
| MK83 B | SACCOACT |

**Table S3.** Weapon types and corresponding source database for the weapon types used in the analysis.

| Category | Craters | Pattern | Rim | Group | Crescent | Bowl | Number of Weapons |
|---|---|---|---|---|---|---|---|
| Total bombing[5] | 0.58 | 0.55 | 0.46 | 0.33 | 0.61 | 0.41 | 2,232,280 |
| Bombing previous year | 0.76 | 0.74 | 0.78 | 0.68 | 0.52 | 0.62 | 654,730 |
| Kinetic weapons[6] over 200 pounds | 0.58 | 0.55 | 0.46 | 0.34 | 0.62 | 0.42 | 2,364,961 |
| Kinetic weapons over 200 pounds previous year | 0.76 | 0.74 | 0.78 | 0.69 | 0.51 | 0.62 | 713,599 |
| Kinetic weapons under 200 pounds | 0.12 | 0.10 | 0.02 | -0.07 | 0.29 | 0.10 | 316,442 |
| Kinetic weapons under 200 pounds previous year | 0.52 | 0.50 | 0.54 | 0.48 | 0.35 | 0.45 | 15,472 |
| Non-kinetic weapons[7] | 0.26 | 0.24 | 0.20 | 0.05 | 0.31 | 0.22 | 52,238 |
| Non-kinetic weapons previous year | 0.38 | 0.36 | 0.35 | 0.27 | 0.27 | 0.32 | 5,111 |
| Unknown weapon type | 0.76 | 0.74 | 0.71 | 0.61 | 0.60 | 0.58 | 702,797 |
| Unknown weapon type previous year | 0.77 | 0.74 | 0.79 | 0.69 | 0.52 | 0.64 | 489,716 |
| B-52 SACCOACT previous year | 0.72 | 0.70 | 0.73 | 0.68 | 0.48 | 0.54 | 438,411 |
| B-52 SEADAB previous year | 0.73 | 0.71 | 0.75 | 0.70 | 0.49 | 0.56 | 456,992 |
| B-52 SACCOACT | 0.53 | 0.50 | 0.44 | 0.36 | 0.51 | 0.36 | 1,210,553 |
| B-52 SEADAB | 0.68 | 0.69 | 0.61 | 0.53 | 0.56 | 0.44 | 687,490 |

**Table S4.** Spearman correlation coefficients between detected craters and number of weapons dropped according to the THOR bombing data aggregated across grid cells of 2 km × 2km in the Quang Tri study area. The number of weapons dropped based on the THOR data is provided for additional context. For the "Craters" category detected craters of all crater classes were aggregated before calculating the correlation. The descriptor

[5] Total bombing refers to the final processing of the THOR data for our analysis, as presented in the paper itself, and therefore only considers the weapon types in Table S2

[6] Kinetic weapons refer to the classification provided by the *mfunc_desc_class* column. Here we consider the B-52 bombings with mission function code 61 originating from the SEADAB data as kinetic despite them being classified as non-kinetic in THOR. However, we did not update any other wrongly mapped mission function codes (see Text S2 Part 2 for details). No other filters, such as selecting specific weapon types (Text S2 Part 5) or removing records with too many bombs per plane (Text S2 Part 6) were applied.

[7] Non-kinetic weapons refer to the classification provided by the *mfunc_desc_class* column. We consider the B-52 bombing missions originating from SEADAB as kinetic and therefore exclude them here. No other filters were applied. Case numbers are low as most non-kinetic missions record 0 for the *numweaponsdelivered* field.

"previous year" was added where only missions that took place during the year before the KH-9 images were taken were considered, otherwise all missions before the KH-9 images were taken were considered.

| Category | Craters | Pattern | Rim | Group | Crescent | Bowl | Number of Weapons |
|---|---|---|---|---|---|---|---|
| Bombing | 0.52 | 0.52 | 0.4 | 0.1 | 0.45 | 0.33 | 1,133,025 |
| Bombing previous year | 0.51 | 0.53 | 0.42 | 0.11 | 0.47 | 0.33 | 321,504 |
| Kinetic weapons over 200 pounds | 0.52 | 0.52 | 0.4 | 0.1 | 0.45 | 0.34 | 1,250,068 |
| Kinetic weapons over 200 pounds previous year | 0.51 | 0.52 | 0.41 | 0.12 | 0.46 | 0.32 | 343,853 |
| Kinetic weapons under 200 pounds | 0.41 | 0.4 | 0.32 | 0.09 | 0.35 | 0.29 | 534,798 |
| Kinetic weapons under 200 pounds previous year | 0.34 | 0.34 | 0.29 | 0.13 | 0.29 | 0.25 | 149,409 |
| Non-kinetic weapons | 0.17 | 0.18 | 0.13 | 0.07 | 0.14 | 0.1 | 78,338 |
| Non-kinetic weapons previous year | 0.12 | 0.13 | 0.1 | 0.08 | 0.11 | 0.07 | 3,011 |
| Unknown weapon type | 0.49 | 0.49 | 0.39 | 0.11 | 0.43 | 0.34 | 600,066 |
| Unknown weapon type previous year | 0.5 | 0.5 | 0.4 | 0.12 | 0.44 | 0.32 | 334,623 |
| B-52 SACCOACT previous year | 0.43 | 0.44 | 0.38 | 0.07 | 0.4 | 0.3 | 220,174 |
| B-52 SEADAB previous year | 0.46 | 0.47 | 0.38 | 0.1 | 0.43 | 0.31 | 239,741 |
| B-52 SACCOACT | 0.47 | 0.48 | 0.38 | 0.08 | 0.43 | 0.31 | 711,533 |
| B-52 SEADAB | 0.48 | 0.49 | 0.4 | 0.09 | 0.44 | 0.33 | 294,806 |

**Table S5.** Spearman correlation coefficients between detected craters and number of weapons dropped according to the THOR bombing data aggregated across grid cells of 2 km × 2km in the Tri-border study area. The number of weapons dropped based on the THOR data is provided for additional context. For the "Craters" category detected craters of all crater classes were aggregated before calculating the correlation. The descriptor "previous year" was added where only missions that took place during the year before the KH-9 images were taken were considered, otherwise all missions before the KH-9 images were taken were considered.

**References:**


Aschauer, J., & Kenkmann, T. (2017). Impact cratering on slopes. *Icarus*, *290*, 89–95. https://doi.org/10.1016/j.icarus.2017.02.021

Barlow, N. G., Stopar, J. D., & Hargitai, H. (2021). Ejecta (Impact). In H. Hargitai & Á. Kereszturi (Eds.), *Encyclopedia of Planetary Landforms* (pp. 1–8). New York, NY: Springer New York. https://doi.org/10.1007/978-1-4614-9213-9_114-1

Duncan, E. C., Skakun, S., Kariryaa, A., & Prishchepov, A. V. (2023). Detection and mapping of artillery craters with very high spatial resolution satellite imagery and deep learning. *Science of Remote Sensing*, *7*, 100092–100092. https://doi.org/10.1016/j.srs.2023.100092

Hayashi, K., & Sumita, I. (2017). Low-velocity impact cratering experiments in granular slopes. *Icarus*, *291*, 160–175. https://doi.org/10.1016/j.icarus.2017.03.027

Lin, E., Qin, R., Edgerton, J., & Kong, D. (2020). Crater detection from commercial satellite imagery to estimate unexploded ordnance in Cambodian agricultural land. *PLOS ONE*, *15*(3), e0229826. https://doi.org/10.1371/journal.pone.0229826

Roberts, A. L., Fawdon, P., & Mirino, M. (2021). Impact crater degradation, Oxia Planum, Mars. *Journal of Maps*, *17*(2), 581–590. https://doi.org/10.1080/17445647.2021.1976685

Sabuwala, T., Butcher, C., Gioia, G., & Chakraborty, P. (2018). Ray Systems in Granular Cratering. *Physical Review Letters*, *120*(26), 264501–264501. https://doi.org/10.1103/PhysRevLett.120.264501